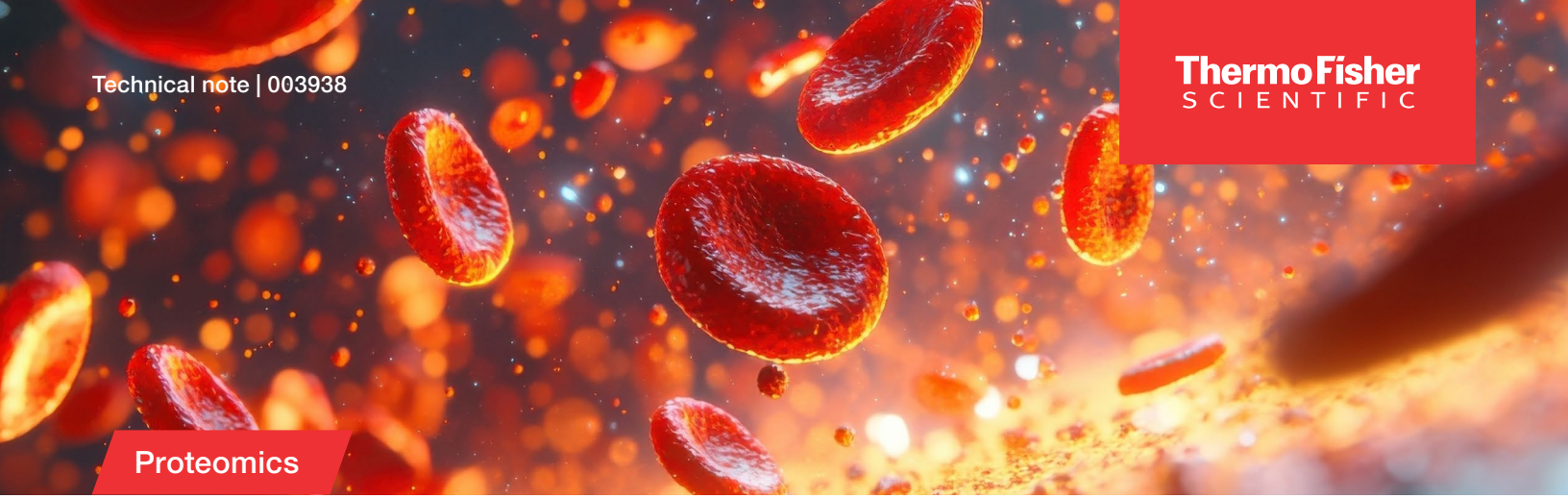

Technical note | 003938

Proteomics

Uncovering biological differences at scale

High-throughput and in-depth plasma proteomics with the Seer Proteograph ONE workflow and Orbitrap Astral Zoom mass spectrometer

Authors

Sudipa Maity[1], Jared Deyarmin[1], Jolene Duda[1], Kevin Yang[1], Amirmansoor Hakimi[1], Stephanie Samra[1], Lee Cantrell[2], Xiaoyan Zhao[2], Taylor Page[2]

[1]Thermo Fisher Scientific, San Jose, CA

[2]Seer Inc., Redwood City, CA

Keywords

Orbitrap Astral Zoom MS, Vanquish Neo UHPLC system, Proteograph ONE, biomarker discovery, plasma proteomics, colorectal cancer, Alzheimer's disease, lung cancer

Goal

Demonstrate how the combination of the Seer® Proteograph® ONE workflow with the Thermo Scientific™ Orbitrap™ Astral™ Zoom mass spectrometer enables deep, quantitative, and reproducible profiling of the plasma proteome. By overcoming challenges such as high dynamic range and low-abundance protein detection, this end-to-end workflow supports the discovery of biologically and clinically relevant biomarker candidates, offering new insights into systemic processes and disease progression for future large-scale translational and clinical research.

Introduction

Plasma proteomics—the large-scale study of proteins in blood plasma—has emerged as a powerful tool in modern biological studies and precision medicine. Its minimally invasive nature and broad coverage of circulating proteins make it ideal for discovering biomarkers and uncovering molecular signatures associated with disease onset, progression, and pharmaceutical response.[1] By capturing dynamic changes in protein abundance, plasma proteomics provides a window into systemic biological processes related to disease biology.

Despite its promise, plasma proteomics faces a fundamental challenge with the large dynamic range of plasma protein concentrations, which is still an obstacle to identifying and quantifying proteins.[2] High-abundance proteins such as albumin and immunoglobulins dominate the plasma proteome, often masking lower-abundance proteins that are biologically significant, especially early-stage disease markers.[3] Additionally, variability in sample collection, preparation, and analysis introduces noise that can obscure true biological signals, limiting reproducibility and the translation of findings into clinical applications.[4]

To overcome the limitations of traditional plasma proteomics—such as poor reproducibility, limited depth, and insufficient detection of low-abundance proteins—we integrated the Proteograph ONE workflow with the Orbitrap Astral Zoom mass spectrometer. This unique combination offers an unbiased, nanoparticle-based enrichment strategy[2] paired with ultra-sensitive, high-throughput mass spectrometry, enabling deep, quantitative plasma proteome profiling while enhancing detection of key proteins and pathways for robust biomarker discovery and disease insights.

Unlike alternative workflows, the Proteograph ONE workflow and Orbitrap Astral Zoom MS combination offers end-to-end sample preparation automation, high reproducibility, and flexible throughput options. The use of Seer's proprietary engineered nanoparticles improves low-abundance protein capture, while the Thermo Scientific™ Vanquish™ Neo UHPLC system and Orbitrap Astral Zoom MS ensure high-resolution, low-flow separation with excellent quantification across the dynamic range of plasma. This superior performance supports both large-scale clinical studies and ultra-deep discovery efforts, setting a new benchmark for scalable, sensitive, and biologically meaningful plasma proteomics (Figure 1).

Experimental

Common consumables

- Water with 0.1% formic acid (FA) (v/v), Optima™ LC-MS grade, Fisher Chemical™ (P/N LS118-500)
- 80% Acetonitrile (ACN), 20% water with 0.1% formic acid, Optima™ LC-MS, Fisher Chemical™ (P/N LS122500)

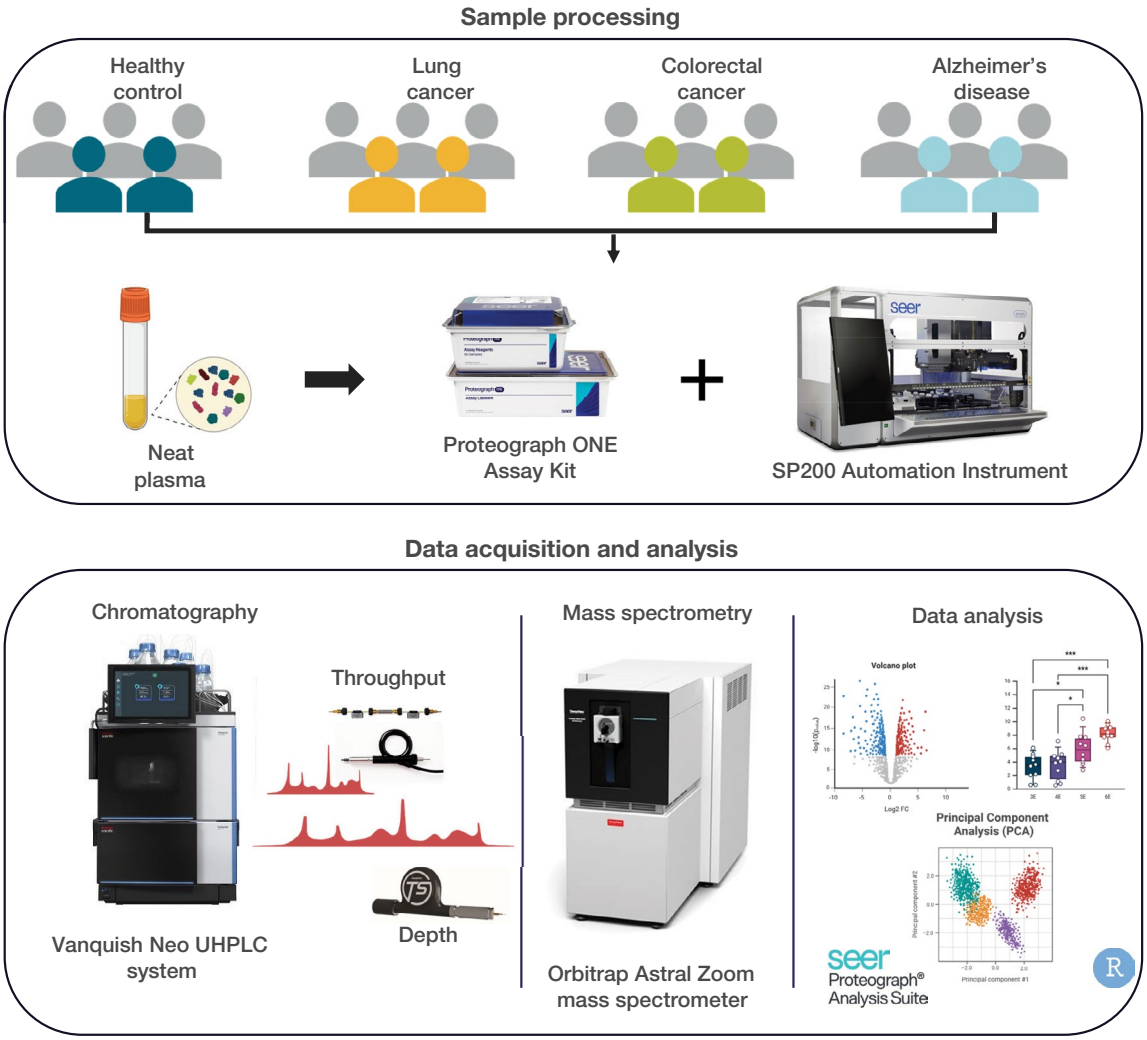

Figure 1. Transforming plasma proteomics and unveiling biological insights with the Proteograph ONE workflow and Orbitrap Astral Zoom mass spectrometer. Created with Biorender.com.

- Formic acid, 99.0+%, Optima™ LC-MS grade, Fisher Chemical™ (P/N A117-50)
- Thermo Scientific™ Pierce™ Quantitative Fluorometric Peptide Assay Kit (P/N 23290)
- Thermo Scientific™ SureSTART™ 9 mm screw caps (P/N 6PSC9STB1)
- Thermo Scientific™ SureSTART™ 0.2 mL TPX screw top microvial with glass insert (P/N 60180-1655)
- Seer® Proteograph® ONE Assay Kit

LC analytical and trap columns

- Thermo Scientific™ EASY-Spray™ HPLC column, 2 µm C18 150 µm × 15 cm (P/N ES906)
- IonOpticks Aurora® Frontier™ 60 × 75 C18 UHPLC column (P/N AUR3-60075C18)
- Thermo Scientific™ PepMap™ Neo Trap Cartridge, 5 µm C18 300 µm × 5 mm (P/N 174500)

Instrumentation

- Thermo Scientific™ Savant SpeedVac™ Concentrator
- Vanquish Neo UHPLC system
- Orbitrap Astral Zoom mass spectrometer
- Seer SP200 automation instrument

Sample preparation

K_2EDTA human plasma samples from healthy controls and age- and gender-matched subjects with lung cancer, colorectal cancer, and Alzheimer's disease were procured from BioIVT. Blood samples were separated into plasma using standardized plasma separation protocols. Single-spun plasma was used for healthy controls, lung cancer, and Alzheimer's disease samples, while double-spun plasma was used for colorectal cancer samples, based on sample availability. Plasma peptides were then prepared using the SP200 Automation Instrument with the Proteograph ONE workflow. Specifically, 120 µL of plasma sample was loaded onto the SP200 instrument and 100 µL was automatically mixed with the nanoparticles included in the Proteograph ONE Assay Kit. Sample-nanoparticle mixtures were incubated for one hour (37 °C) for protein corona formation based on physicochemical properties of the particles. A series of washes were performed to remove non-specific and weakly bound proteins. Plasma proteins bound to nanoparticles were then reduced, alkylated, and digested with Trypsin/Lys-C. Digested peptides underwent cleanup and desalting using a particle-based system. Eluted peptides were quantified using the Pierce Quantitative Fluorometric Peptide Assay Kit. Peptides were then dried down with a Savant SpeedVac concentrator and reconstituted in water with 0.1% formic acid and 3% acetonitrile to a final concentration of 50 ng/µL. Five hundred nanograms of peptide mass was loaded on the column for LC-MS analysis across all throughputs.

LC-MS analysis

All LC-MS runs for Proteograph ONE-processed plasma peptides were separated and analyzed using a Vanquish Neo UHPLC system coupled to an Orbitrap Astral Zoom mass spectrometer. Peptide separation was achieved on the Vanquish Neo UHPLC system using either a trap-and-elute configuration with an EASY-Spray analytical column (15 cm, 150 µm, 2 µm particle size) or a direct injection configuration with an Aurora Frontier C18 UHPLC column (60 cm, 75 µm, 1.7 µm particle size). Chromatographic gradients were formed using 0.1% formic acid in water as mobile phase A and 0.1% formic acid in 80% acetonitrile as mobile phase B. Detailed liquid chromatography parameters and gradient settings are provided in Table 1. Mass spectrometer source parameters and scan parameters can be found in Table 2.

Table 1A. Vanquish Neo UHPLC system gradients and LC parameters for 60 SPD throughputs. 60 SPD sample separation was performed with a trap-elute configuration.

60 SPD		
Gradient		
Time (min)	% Mobile phase B	Flow (µL/min)
0	10	2.0
0.3	10	2.0
0.6	10	0.8
13.6	22.5	0.8
20.5	35.0	0.8
20.9	55.0	2.0
20.95	99.0	2.0
22.35	99.0	2.0
LC parameters		
LC configuration	Trap and Elute	
Fast loading/equilibration mode	Pressure Control	
Loading/equilibration/wash pressure	Max Pressure	
Equilibration factor	3	
Sampler temperature (°C)	7	
Mobile phase A / weak wash	0.1% Formic acid in water	
Mobile phase B / strong wash	0.1% Formic acid in 80% acetonitrile	
Zebra wash	Enabled	
Zebra wash cycles	4	
Analytical column temperature (°C)	50	
Column specifications		
Analytical column	EASY-Spray HPLC column, 2 µm C18, 150 µm × 15 cm (P/N ES906)	
Trap column	PepMap Neo Trap Cartridge, 5 µm C18 300 µm x 5 mm, (P/N 174500)	

Table 1B. Vanquish Neo UHPLC system gradients and LC parameters for 16 SPD throughputs. 16 SPD sample separation was performed with a direct configuration.

16 SPD		
Gradient		
Time (min)	% Mobile phase B	Flow (µL/min)
0	8	0.25
1.0	8	0.25
1.5	8	0.2
61.5	28.0	0.2
78.5	50.0	0.2
79.0	99.0	0.4
81.5	99.0	0.4
83.5	99.0	0.4
LC parameters		
LC configuration	Direct	
Fast loading/equilibration mode	Pressure Control	
Loading/equilibration/wash pressure	Max Pressure	
Equilibration factor	2	
Sampler temperature (°C)	7	
Mobile phase A / weak wash	0.1% Formic acid in water	
Mobile phase B / strong wash	0.1% Formic acid in 80% acetonitrile	
Zebra wash	Not enabled	
Zebra wash cycles	0	
Analytical column temperature (°C)	55	
Column specifications		
Analytical column	Aurora Frontier C18 UHPLC column, 1.7 µm C18, 75 µm × 60 cm (P/N AUR3-60075C18)	

Table 2A. Orbitrap Astral Zoom mass spectrometer parameters: Global source and mass spectrometer parameters

Global parameters (source & MS)	
Positive ion voltage (V)	2,100
Ion transfer tube temperature (°C)	290
Expected peak width (s)	10
Default charge state	2
Lock mass correction	Off

Table 2B. Orbitrap Astral Zoom mass spectrometer parameters: MS1 full scan experiment parameters

MS1 full scan experiment parameters	
Orbitrap resolution	240K
Scan range (*m/z*)	380–980
Normalized AGC target (%) / Absolute AGC value	500% / 5.00e6
Maximum injection time (ms)	5
Microscans	1
RF lens (%)	40

Table 2C. Orbitrap Astral Zoom mass spectrometer parameters: MS2 DIA scan experiment parameters

MS2 DIA scan experiment parameters	
Precursor mass range (*m/z*)	380–980
Isolation window (*m/z*)	2.5 (16 SPD) or 3 (60 SPD)
Window placement optimization	On
AGC target	Custom
Normalized AGC target (%) / Absolute AGC value	500% / 5.00e4
Maximum injection time (ms)	7
DIA scan range (*m/z*)	150–2,000
HCD collision energy (%)	25
RF lens (%)	40
Pre-accumulation	On
Loop control	Time
Time (s)	0.6

Data processing and analysis

All acquired LC-MS data was processed using library-free analysis without match between runs (MBR) using DIA-NN (version 1.8.1) in the Proteograph® Analysis Suite (PAS) (Seer Inc). All results were processed and filtered with a 1% precursor and 1% protein group false discovery rate (FDR). Exported output files were imported to RStudio™ (2023.09.0 Build 463) with R (v4.3.1) for downstream data analysis and visualization.

Results and discussion

Performance with the Proteograph ONE workflow and Orbitrap Astral Zoom MS

To evaluate analytical measurement precision and identification depth, pooled healthy plasma samples were processed in triplicate and analyzed using two LC-MS methods (Figure 2): a high-throughput 60 samples per day (SPD) workflow and a deeper-coverage 16 SPD workflow. As shown in Figure 2A, the 16 SPD method achieved higher overall identifications, with a median of 9,047 protein groups and 116,379 peptides. The 60 SPD method, while yielding slightly fewer identifications (6,770 protein groups and 69,146 peptides), still delivered substantial proteome coverage. Notably, both methods demonstrated excellent technical reproducibility. Figure 2B shows median coefficients of variation (%CV) across technical replicates, with protein %CVs of only 4.2% (60 SPD) and 4.3% (16 SPD), and peptide %CVs of 8.1% and 8.9%, respectively. These results highlight that while the 16 SPD method is optimized for maximum depth, the 60 SPD method strikes an effective balance between throughput and depth—offering robust protein and peptide identification alongside consistent measurement precision, making it highly suitable for large-scale studies.

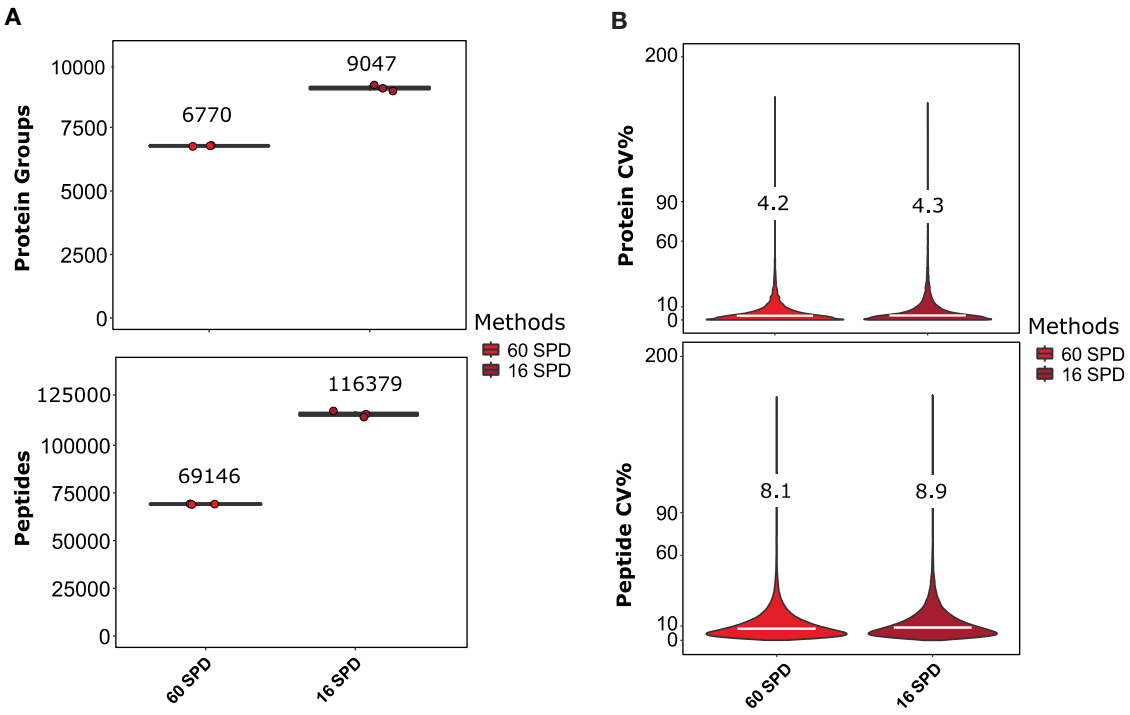

Figure 2. Analytical measurement precision from plasma sample preparation technical replicates. (A) Box plots show protein (top) and peptide (bottom) identifications from triplicate independent preparations of pooled healthy plasma with single injections on the Orbitrap Astral MS across different throughputs. Conditions are ordered left to right from high throughput (60 SPD, red) to maximum depth (16 SPD, dark red), with medians indicated by black lines and values. Circles represent individual sample preparation technical replicate injections. (B) Violin plots show protein (top) and peptide (bottom) %CV across the same triplicates, with median %CVs indicated.

Protein and peptide identifications in subject-derived samples and healthy controls

To assess proteome coverage across disease states, protein group and peptide identifications were compared using both high-throughput (60 SPD) and deep-coverage (16 SPD) LC-MS methods across biological conditions (Figure 3). The 60 SPD method enabled comprehensive identification of plasma proteins and peptides across all samples, with a total identification of 8,213 protein groups and 92,873 peptides in the entire study. The 16 SPD method highlights increased depth, yielding a total of 10,769 protein groups and 152,009 peptides. Notably, the 60 SPD method delivered substantial depth across diverse sample types, demonstrating its suitability for large-scale studies where high throughput and scalability are essential. In contrast, the 16 SPD method maximizes proteomic depth, making it ideal for applications that require more comprehensive proteome profiling.

Dynamic range in high-throughput and Max-ID throughput methods

To evaluate the dynamic range of protein quantification, protein groups identified using the 60 SPD (high-throughput) and 16 SPD (deep-coverage) workflows were ranked by average protein abundance and plotted on a logarithmic scale. As shown in the rank plots (Figure 4), both methods demonstrate relative measurements of protein group abundances across 8 to 9 orders of magnitude, enabling detection of plasma proteins across the wide dynamic range. These results emphasize the sensitivity and quantitative power of the Proteograph ONE workflow combined with the Orbitrap Astral Zoom mass spectrometer, regardless of throughput.

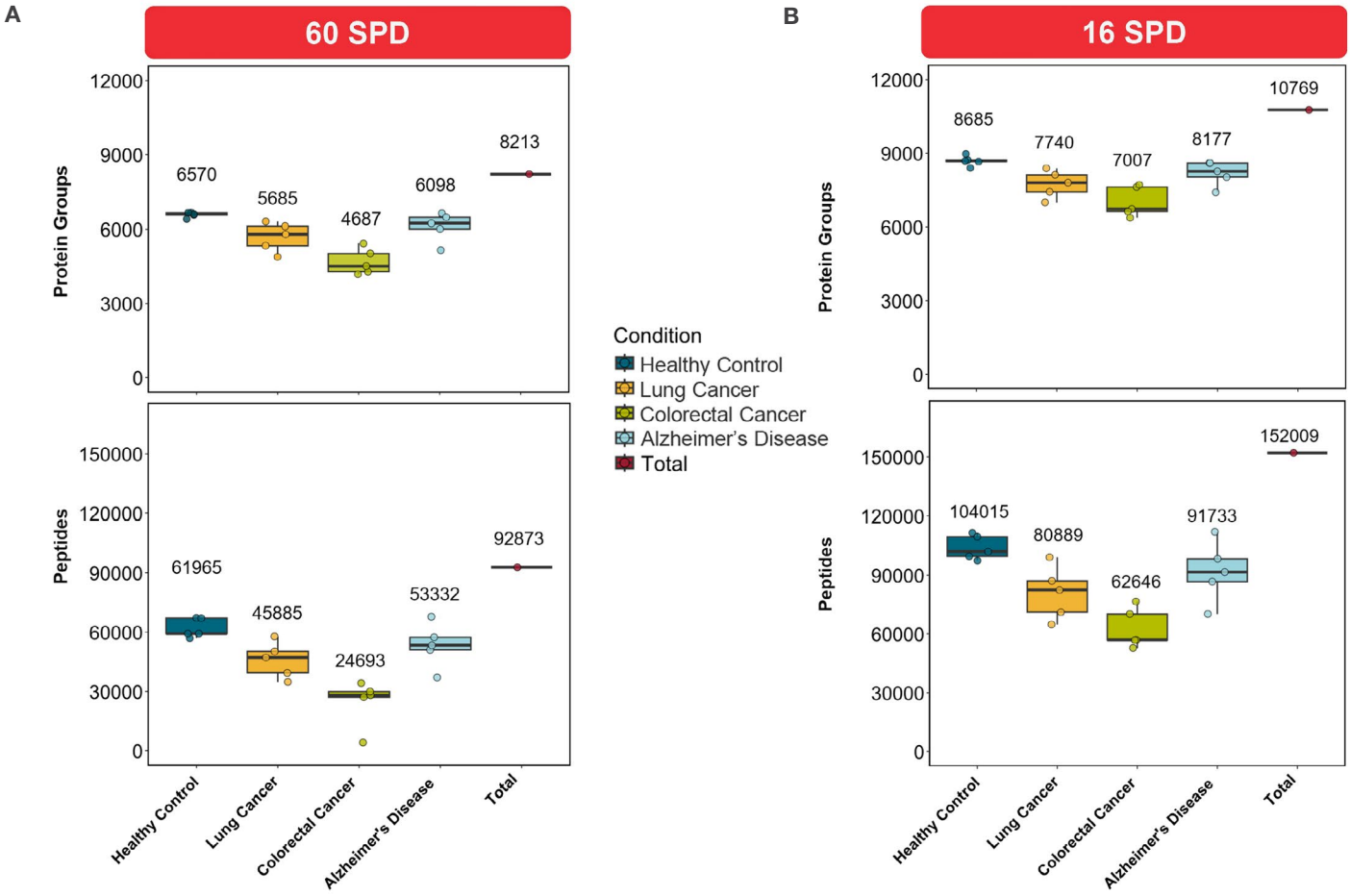

Figure 3. Protein group and peptide identifications across biological sample groups. (A) High-throughput (60 SPD) method and (B) maximum-identification throughput (16 SPD) method. Median protein and peptide numbers are indicated by values above box plots.

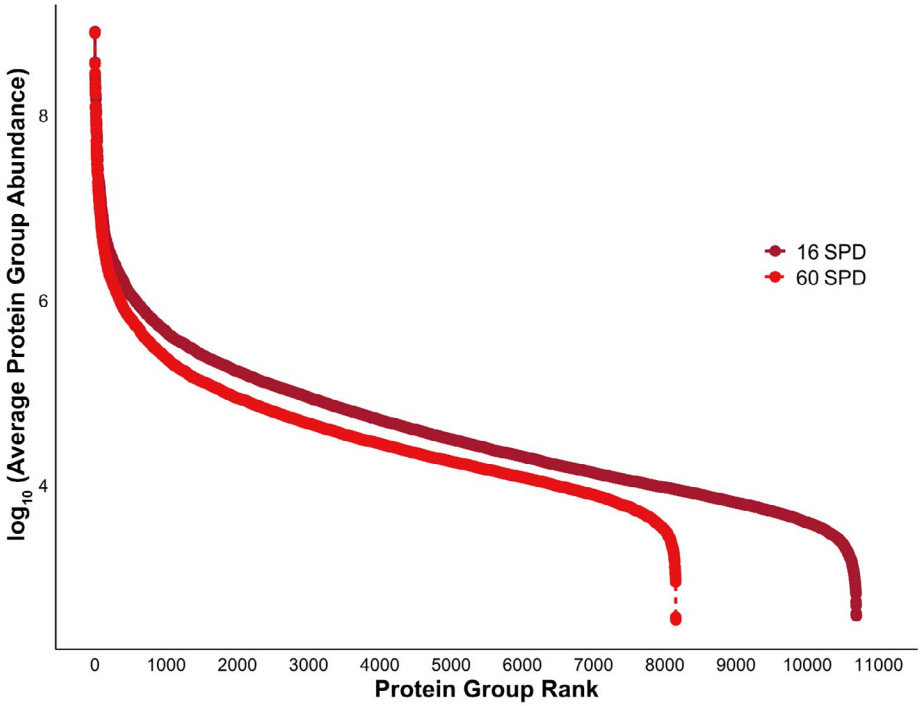

Figure 4. Rank plots across different throughputs. Protein groups from the 60 SPD (red) and 16 SPD (dark red) workflows were ranked on the x-axis, with the y-axis showing $\log_{10}$ of average protein group abundance.

Overlap and coverage of protein identifications between workflows

A Euler diagram comparing 60 SPD and 16 SPD workflows revealed substantial overlap in protein group identifications (Figure 5). Of the total 11,357 protein groups identified across both methods, 7,625 (67%) were shared between the 16 SPD and 60 SPD workflows, highlighting substantial overlap and demonstrating that both methods capture a highly consistent core proteome. The deeper 16 SPD method uniquely identified 3,144 protein groups (28%), while the high-throughput 60 SPD method contributed 588 unique protein groups (5%). Notably, the 60 SPD method recovered approximately 71% of the proteins detected by the 16 SPD workflow, underscoring its ability to achieve broad proteome coverage with 3.75x higher throughput. In addition, the Proteograph ONE workflow captures 74 of the FDA-approved protein biomarkers,[5] highlighting that in addition to added plasma proteome depth, clinically demonstrated protein biomarkers of physiological relevance are also measured (Figure 5).

Distinct proteomic signatures: PCA highlights subject variability and sample preparation and instrument analytical precision

Principal component analysis (PCA) was performed to assess sample clustering and variance across both 60 SPD (Figure 6, left) and 16 SPD (Figure 6, right) workflows. In both cases, healthy control samples (dark blue) exhibited tight clustering with minimal variance along the second principal component (PC2), and their technical replicates (red) clustered closely together, indicating high reproducibility of the Proteograph ONE workflow and Orbitrap Astral Zoom mass spectrometer. In contrast, subject-derived samples displayed broader dispersion across the principal components, reflecting greater proteomic variance consistent with biological heterogeneity and disease-specific molecular differences. This pattern was consistently observed across both throughputs, demonstrating that both workflows capture relevant biological signals while maintaining strong technical reproducibility.

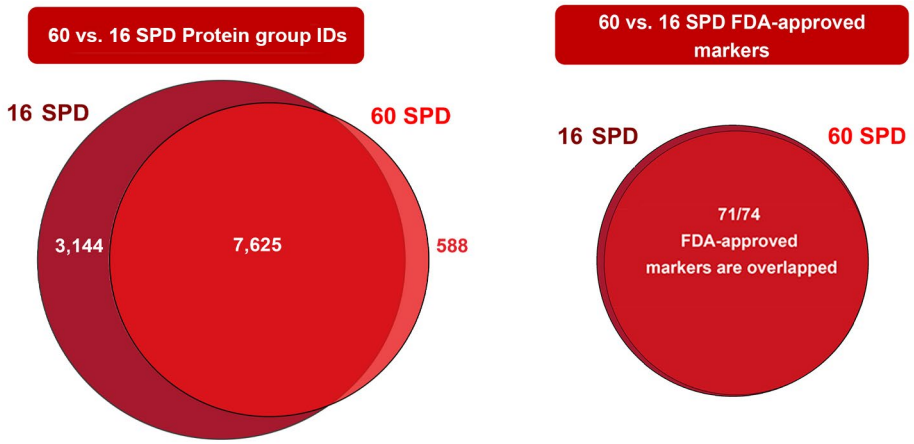

Figure 5. Protein group overlaps between both SPDs and FDA-approved biomarker coverage. Euler diagram (left) depicts protein group overlaps between high-throughput and maximum-identification methods. Euler diagram (right) depicts the FDA-approved biomarker proteins identified between both workflows.

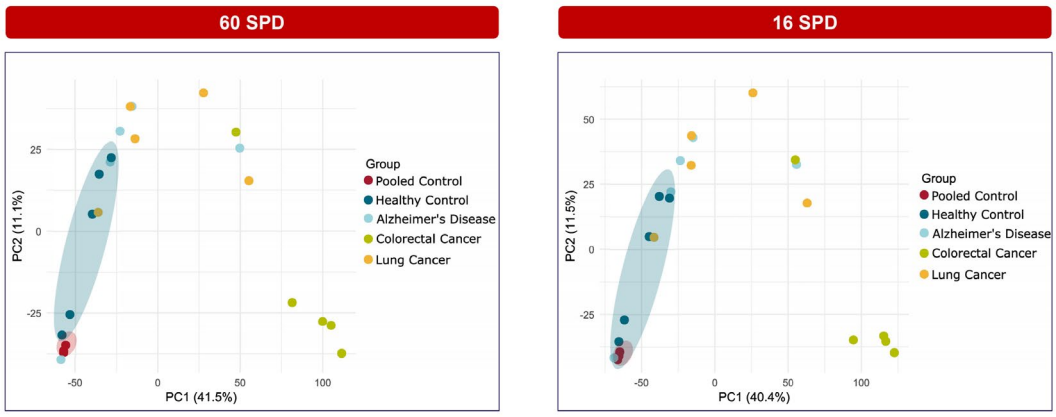

Figure 6. PCA reveals greater variance among patient-derived samples compared to healthy controls. Healthy controls (dark blue) show minimal variance with tightly clustered technical replicates (red), indicating strong instrument reproducibility. Subject samples show broader PCA dispersion, reflecting biological heterogeneity.

Biological signatures linked to variations in protein abundance in lung cancer samples

Plasma proteomic analysis comparing lung cancer subjects to healthy controls revealed over 1,200 differentially expressed proteins (DEPs), with 603 proteins downregulated and 661 upregulated in lung cancer samples (Figure 7). Among the upregulated proteins, several FDA-approved biomarkers were identified (highlighted in dark red), underscoring the ability to detect clinically relevant proteins with the end-to-end workflow. These results demonstrate the platform's ability to sensitively detect disease-associated proteomic alterations and capture potential biomarker candidates directly from plasma, enabling powerful biological and translational insights.

Deep functional insights from differentially abundant proteins

Many of the gene ontology (GO) and Reactome enriched pathways—such as those involved in immune signaling, chemotaxis, wound healing, cell migration, tissue remodeling, and hemostasis—are closely linked to known mechanisms of lung cancer progression.[6-8] The distinct enrichment patterns observed demonstrate the ability of the end-to-end workflow to detect biologically meaningful alterations between disease and healthy states (Figure 8). This highlights the potential of the platform for uncovering clinically relevant biomarkers and gaining mechanistic insights into disease biology.

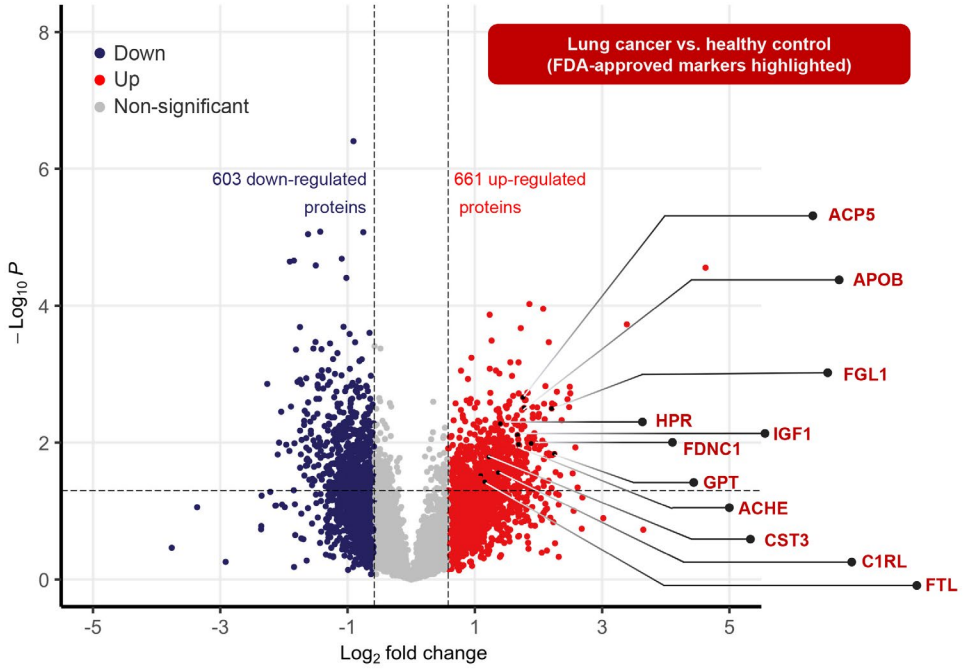

Figure 7. Differentially expressed proteins across lung cancer vs. healthy controls. Over 1,200 proteins were differentially expressed in plasma from lung cancer vs. healthy samples. Some of the protein candidates with higher abundance, highlighted in dark red, include FDA-approved protein biomarkers.

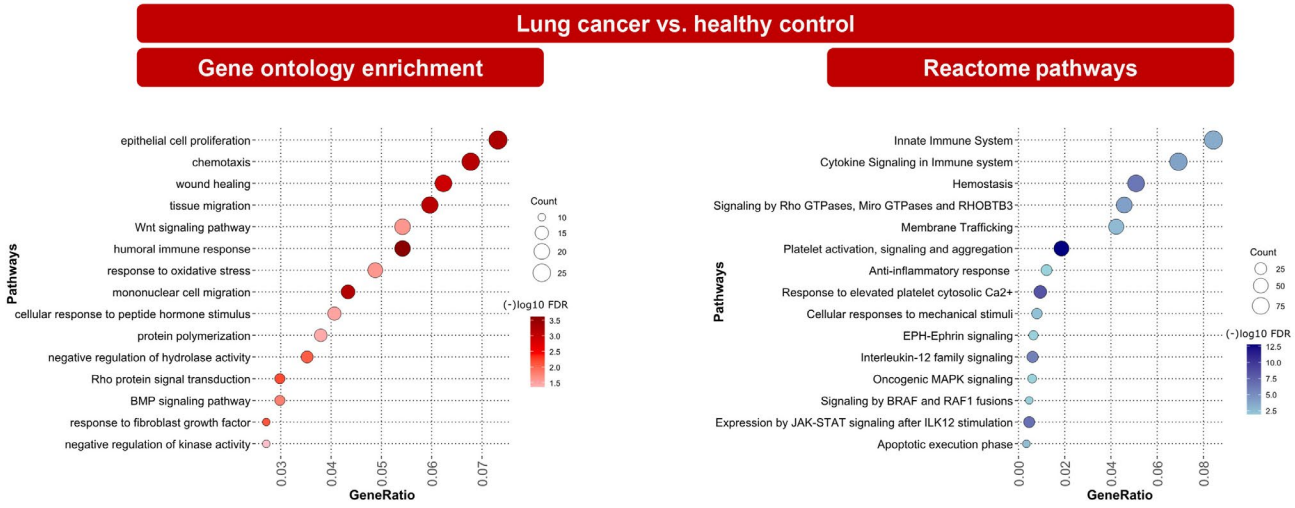

Figure 8. Pathway enrichment analysis. FDR enriched 15 GO (left) and Reactome pathway (right) enrichment analyses of differentially expressed proteins in lung cancer vs. healthy controls highlight dysregulated pathways, with statistical significance (-log$_{10}$ FDR) shown by color and protein count by bubble size. For GO and Reactome pathway enrichment analyses, p-value and q-values were cut off at 0.05 and p-values were adjusted using the Benjamini-Hochberg procedure to control the FDR.

Conclusion

- The Proteograph ONE workflow combined with the Orbitrap Astral Zoom mass spectrometer identified >10,800 protein groups using ultradeep profiling, compared to >8,200 with the high-throughput method—demonstrating scalable, reproducible plasma proteomics with clear detection of biological differences for biomarker discovery applications.
- The Proteograph ONE workflow combined with the Orbitrap Astral Zoom mass spectrometer captures exceptional dynamic range of 7-8 orders of magnitude in plasma proteome.
- >1,000 differentially abundant proteins detected with biologically relevant dysregulated pathways, such as immune signaling or tissue remodeling, underscore the complex biology of lung cancer.
- Identification of FDA markers as differentially expressed showcases the workflow's strength for capturing biologically relevant plasma proteins.

References

1. Ignjatovic, V. *et al.* Mass spectrometry-based plasma proteomics: Considerations from sample collection to achieving translational data. *J. Proteome Res.* **2019,** *18,* 4085.
2. Blume, J. E. *et al.* Rapid, deep and precise profiling of the plasma proteome with multi-nanoparticle protein corona. *Nat. Commun.* **2020,** *11,* 3662.
3. Geyer, P. E. *et al.* Plasma proteome profiling to detect and avoid sample-related biases in biomarker studies. *EMBO Mol. Med.* **2019,** *11.*
4. Geyer, P. E. *et al.* The circulating proteome—Technological developments, current challenges, and future trends. *J. Proteome Res.* **2024,** *23,* 44.
5. Anderson, N.L. The clinical plasma proteome: a survey of clinical assays for proteins in plasma and serum. *Clin. Chem.* **2010** Feb, *56*(2), 177–85.
6. Muliaditan, T. *et al.* Macrophages are exploited from an innate wound healing response to facilitate cancer metastasis. *Nat. Commun.* **2018,** *9,* 1.
7. Friedl, P.; Wolf, K. Tumour-cell invasion and migration: Diversity and escape mechanisms. *Nat. Rev. Cancer* **2003,** 362.
8. Greenwell, J. C.; Torres-Gonzalez, E.; Ritzenthaler, J. D.; Roman, J. Interplay between aging, lung inflammation/remodeling, and fibronectin EDA in lung cancer progression. *Cancer Biol. Ther.* **2020,** *21,* 1109.

Learn more at **thermofisher.com/orbitrapastralzoom**